



OPEN ACCESS

EDITED BY Petru Liuba, Lund University, Sweden

REVIEWED BY
Jorge Aramburu,
University of Navarra, Spain
Gyu-Han Lee,
Flonics Co., Ltd., Republic of Korea

*CORRESPONDENCE
Sebastian Laudenschlager

■ sebastian.laudenschlager@hsc.wvu.edu

RECEIVED 03 September 2025 ACCEPTED 17 October 2025 PUBLISHED 05 November 2025

CITATION

Laudenschlager S, Chauhan D, Chaudhuri NR, Mascio CE, Udassi JP, Frank BS, Romanowicz J, Loke Y-H, Kheyfets VO and Hedjazi Moghari M (2025) Estimation of pre-Fontan pulmonary vascular resistance in children with single ventricle heart disease at the Glenn stage: a multicenter study. Front. Pediatr. 13:1698653. doi: 10.3389/fped.2025.1698653

COPYRIGHT

© 2025 Laudenschlager, Chauhan, Chaudhuri, Mascio, Udassi, Frank, Romanowicz, Loke, Kheyfets and Hedjazi Moghari. This is an open-access article distributed under the terms of the Creative Commons Attribution License (CC BY). The use, distribution or reproduction in other forums is permitted, provided the original author(s) and the copyright owner(s) are credited and that the original publication in this journal is cited, in accordance with accepted academic practice. No use, distribution or reproduction is permitted which does not comply with these terms.

Estimation of pre-Fontan pulmonary vascular resistance in children with single ventricle heart disease at the Glenn stage: a multicenter study

Sebastian Laudenschlager^{1*}, Dhaval Chauhan¹, Nita Ray Chaudhuri¹, Christopher E. Mascio¹, Jai P. Udassi¹, Benjamin S. Frank², Jennifer Romanowicz², Yue-Hin Loke³, Vitaly O. Kheyfets^{2,4,5,6} and Mehdi Hedjazi Moghari¹

¹Department of Pediatrics, West Virginia University and West Virginia University Medicine Children's Hospital, Morgantown, WV, United States, ²Department of Cardiology, University of Colorado and Children's Hospital Colorado, Aurora, CO, United States, ³Department of Cardiology, George Washington University and Children's National Hospital, Washington, DC, United States, ⁴Cardiovascular Pulmonary Research Laboratories, Division of Pulmonary Sciences and Critical Care Medicine, Department of Medicine, University of Colorado Anschutz Medical Campus, Aurora, CO, United States, ⁵Division of Pediatrics-Critical Care, Department of Pediatrics, University of Colorado Anschutz Medical Campus, Aurora, CO, United States, ⁵Department of Biomedical Informatics, University of Colorado Anschutz Medical Campus, Aurora, CO, United States

The Fontan procedure, employed in the management of children with single ventricle congenital heart disease, continues to present long-term complications. Notably, certain complications associated with this procedure are linked to imbalances in the distribution of hepatic blood flow. One promising strategy to address this challenge involves employing a digital twin to simulate diverse Fontan configurations. The objective is to identify an optimal design that ensures balanced hepatic blood flow and minimizes power losses. However, successful implementation depends on accurate, patient-specific estimates of pulmonary vascular resistance (PVR) for each lung at the pre-Fontan (Glenn) stage. In clinical practice, only the total PVR is typically measured, via catheterization using the Fick principle, but individual lung resistances can be derived by combining pressure data from catheterization (Cath) with flow data from cardiac magnetic resonance imaging (CMR). Still, notable discrepancies exist: Fick-based total PVR often differs significantly from Cath-CMR-based PVR due to differences in flow quantification, and neither method can distinguish between proximal and distal resistances within the Glenn pathway. An alternative method for estimating PVR was previously developed using a computational fluid dynamics (CFD) optimization framework. This method demonstrated a favorable correlation with PVR estimates derived from Cath-CMR, although it was not directly compared to clinical PVR values derived using the Fick principle. In this study, we compare three methods for calculating PVR, namely Fick-based, Cath-CMR-based, and CFD-based, using patient data from three independent institutions. Our results show that Fick-based PVR values are, on average, significantly lower than those obtained via the Cath-CMR and CFD methods. The CFD-based total PVR estimates show good agreement with the total Cath-CMR-based PVR. However, the elevated left proximal resistance present in the CFD method leads to a significant

underestimation of the left lung resistance by the Cath-CMR method. This underscores the significance of incorporating proximal resistance in PVR estimation and supports the potential utility of the CFD-based method for preoperative planning in single ventricle patients.

KEYWORDS

pulmonary vascular resistance, Fontan surgery, computational fluid dynamics, cardiovascular magnetic resonance, catheterization

1 Introduction

Single ventricle congenital heart disease is typically managed through a three-stage surgical palliation designed to separate the systemic and pulmonary circulations, thereby bypassing the underdeveloped or nonfunctional ventricle (1). This staged approach reduces the mixing of oxygenated and deoxygenated blood, resulting in improved systemic oxygenation. The surgical stages of palliation consist of: (1) stage 1 palliation or the Norwood procedure, (2) the bidirectional Glenn or hemi-Fontan procedure, and (3) the Fontan completion. Following complete palliation, a total cavopulmonary connection (TCPC) is established in which the superior and inferior vena cavae (SVC and IVC) are directly anastomosed to the left and right pulmonary arteries (LPA and RPA). This anatomical configuration enables passive, non-pulsatile pulmonary perfusion, bypassing the need for a subpulmonary ventricle (2).

While this staged palliation has significantly improved survival, long-term complications remain prevalent (3). Many of these are linked to the suboptimal hemodynamic performance of the TCPC (4, 5), including elevated power loss, which contributes to diminished exercise tolerance (6), and the development of pulmonary arteriovenous malformations (7, 8).

One strategy to optimize post-Fontan hemodynamics involves the use of patient-specific computational fluid dynamics (CFD) models to simulate surgical outcomes and predict the effects of alternative TCPC geometries (9, 10). A critical input to such simulations is an accurate estimate of pulmonary vascular resistance (PVR) in each lung prior to Fontan completion. However, in clinical practice, individual lung PVRs are rarely measured; only total PVR is typically derived during cardiac catheterization (Cath), using pressure measurements and pulmonary flow (Q_p) calculated via the Fick principle (11).

Unfortunately, Fick-based estimates of pulmonary flow have been shown to be inconsistent and less reliable than measurements obtained from cardiac magnetic resonance imaging (CMR), particularly in single ventricle patients (12, 13). As a result, Fick-derived total PVR values may lack accuracy. One aim of this study is to quantify the discrepancy between Fick-based and Cath-CMR-based PVR measurements using patient data from three independent institutions. Another limitation of the Fick-based method for estimating PVR is its inability to provide separate left and right lung resistances, as it only calculates the total lung PVR.

While Cath pressure data combined with CMR flow can be used to estimate individual lung PVRs, this method does not

allow for differentiation between proximal and distal resistances along the Glenn pathway. To address this limitation, a CFD-based optimization framework was previously developed to estimate lung-specific PVRs, including proximal resistance components, at the stage 2 (Glenn) physiology (14). However, this earlier study was limited to a small patient cohort from a single institution.

In this manuscript, we expand upon this prior work by applying the PVR estimation algorithm to a larger, multi-institutional dataset. Our goals are twofold: first, to rigorously compare Fick, Cath-CMR, and CFD-based PVR measurements across three centers, and second, to highlight the importance of the proximal resistances found through the CFD-based PVR estimation framework by benchmarking it against the PVR values derived from the Cath-CMR method.

2 Methods

2.1 Patient demographic data

Clinical data for this three-center study were retrospectively collected and anonymized from three medical institutions over a ten-year period, with approval from the Institutional Review Board (IRB) of each participating center. Due to the retrospective nature of the study, the requirement for informed consent was waived. Data were accessed and analyzed between January 2023 and May 2025. The dataset comprises CMR and Cath data from 42 pediatric patients (28 males, 14 females; age range: 2–10 years; mean age 3.85 ± 1.49 years) with Glenn physiology (39 bidirectional Glenn, 3 hemi-Fontan), distributed across the three centers as follows:

- Center 1: 10 males, 6 females; age range: 2–5 years; 13 bidirectional Glenn, 3 hemi-Fontan
- Center 2: 14 males, 6 females; age range: 2-6 years; 20 bidirectional Glenn, 0 hemi-Fontan
- Center 3: 4 males, 2 females; age range: 2–10 years; 6 bidirectional Glenn, 0 hemi-Fontan

CMR imaging was used to construct three-dimensional anatomical models for CFD simulations and to quantify time-averaged pulmonary blood flow in the SVC, LPA, and RPA, as previously described (14). Cath data included mean pressure measurements at the SVC, LPA, RPA, and left atrium (LA). All but four patients had their CMR and CATH examinations within the same week. Of the remaining four patients, two had

their examinations within a month, one half a year apart, and one a year apart.

2.2 Pulmonary vascular resistance

PVR was calculated using three methods: the Fick principle, Cath-CMR-based estimation, and CFD-based modeling. These calculations were conducted for all 42 patients and compared across the three participating centers. All PVR values are reported as body surface area (BSA)-indexed Wood units (iWU or $WU \cdot m^2$).

2.2.1 Estimation of total PVR using the Fick principle

Total PVR, denoted as R_{total} , is calculated exclusively from data measured by a Cath exam, using a hydraulic analogue of Ohm's law:

$$R_{total} = \frac{\Delta P_{transpulmonary}}{Q_p} = \frac{mPAP - PAWP}{Q_p},$$
 (1)

where mPAP is the mean pulmonary artery pressure, calculated as the average of LPA and RPA pressure measurements, PAWP is the pulmonary artery wedge pressure (an estimate of LA pressure), and Q_p is the pulmonary blood flow. Pulmonary blood flow is determined using the Fick principle, which defines flow as the ratio of oxygen consumption (VO_2) to the arteriovenous oxygen content difference across the pulmonary circulation, which are obtained through Cath. In clinical practice, direct measurement of VO_2 via indirect calorimetry is considered the gold standard. However, this method is often impractical, particularly in pediatric settings or during Cath-based procedures (15). As a result, VO_2 is often estimated using predictive equations based on age, body weight, and occasionally heart rate which has limitations in patients with Glenn vasculature (16).

2.2.2 PVR estimation using pressure measurements from Cath and flow measurements from CMR

Individual left and right lung resistances (R_{LPA} and R_{RPA}) can be calculated directly from clinical measurements, specifically using pressure data from Cath and flow data from CMR:

$$R_{LPA} = \frac{P_{LPA} - P_{LA}}{Q_{LPA}}, \quad R_{RPA} = \frac{P_{RPA} - P_{LA}}{Q_{RPA}},$$
 (2)

where Q_{LPA} and Q_{RPA} represent the flow rates through the LPA and RPA, respectively, as measured by CMR. The corresponding resistances, R_{LPA} and R_{RPA} can then be used to compute the total PVR, equivalent to the LPA and RPA resistance in parallel and analogous to the value obtained using the Fick principle:

$$R_{total} = \frac{R_{LPA} \cdot R_{RPA}}{R_{LPA} + R_{RPA}}.$$
 (3)

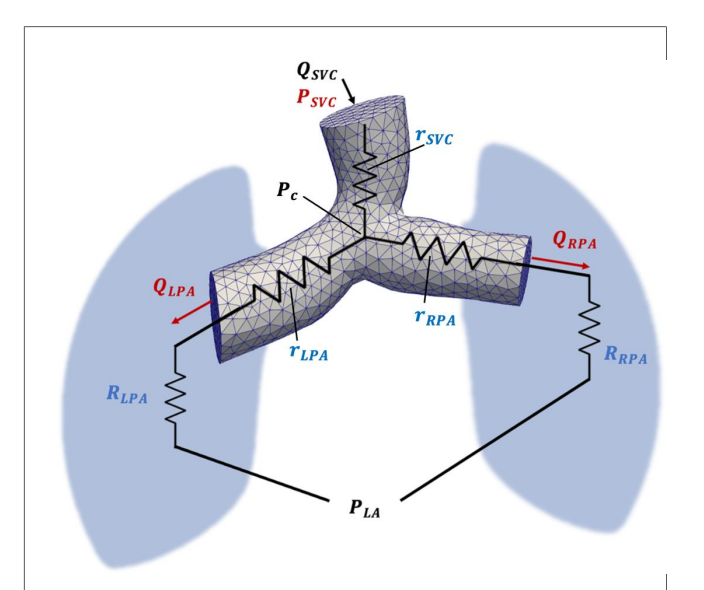


FIGURE 1 Schematic representation of the computational model used for PVR estimation using CFD. Inlet (Q_{SVC}) and outlet (Q_{LPA}, Q_{RPA}) flow is acquired from CMR flow measurements, while SVC, LPA, RPA and LA pressure is acquired from Cath pressure measurements. The pressure at the confluence of the SVC, LPA, and RPA is denoted by $P_{\rm C}$ and was calculated from CFD simulation results. Proximal SVC, LPA, and RPA resistances are denoted as r_{SVC} , r_{LPA} , and r_{RPA} , respectively.

2.2.3 Estimation of PVR using CFD

The individual PVR can also be estimated using a CFD-based optimization algorithm that adjusts the LPA and RPA resistances to minimize the error between simulated and clinical flow and pressure data. This algorithm, implemented using the SimVascular (17) software package, produces separately identifiable distal resistances (R_{LPA} and R_{RPA}), as well as proximal resistances (r_{SVC} , r_{LPA} , and r_{RPA}) corresponding to the SVC, LPA, and RPA, respectively.

The proximal resistances are computed from time-averaged flow rates and pressure gradients derived from the CFD simulation results (Figure 1). The pressure gradients are determined using the average pressure at a point near the center of the confluence of the SVC, LPA, and RPA, denoted as P_c . A detailed description of the PVR estimation algorithm is provided in (14). The proximal resistances can be combined with the distal resistances to account for the resistance along the entire LPA or RPA pathway:

$$\tilde{R}_{LPA} = R_{LPA} + r_{LPA}, \, \tilde{R}_{RPA} = R_{RPA} + r_{RPA}. \tag{4}$$

These combined individual lung resistances can be used in Equation 3 to calculate the total PVR (\tilde{R}_{total}), which is analogous to the value obtained via the Fick principle.

2.3 Statistical analysis

Descriptive statistics for all three centers are presented as mean \pm standard deviation. Normality of the data was assessed using the Shapiro–Wilk test (18). To compare PVR estimates across the three centers, the Kruskal–Wallis rank sum test was employed (19). Paired data were analyzed using Wilcoxon rank sum tests (20), intraclass correlation coefficients (ICC) (21) with 95% confidence intervals (CI), and Bland–Altman analysis (22). A p-value of < 0.05 was considered statistically significant.

3 Results

3.1 Flow and pressure data

Comparison of clinically measured flow values across the three centers using the Kruskal-Wallis test revealed no statistically

significant differences in flow within the SVC, LPA, or RPA (Table 1). In contrast, analysis of pressure measurements obtained via Cath showed significant differences among centers, with Center 1 exhibiting lower mean pressures in the SVC, LPA, RPA, and LA. However, despite these lower absolute pressures in Center 1, the mean pressure gradients in both the LPA $(P_{LPA}-P_{LA})$ and RPA $(P_{RPA}-P_{LA})$, did not differ significantly between centers.

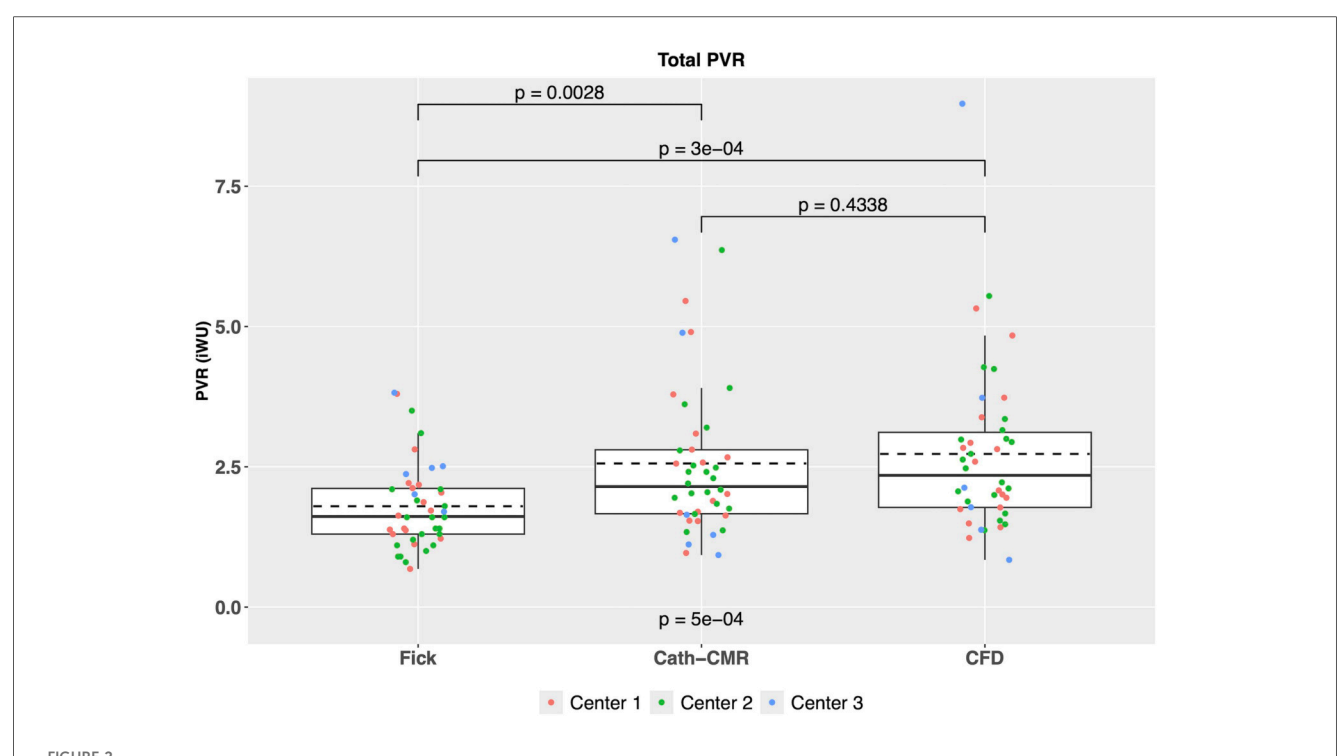
3.2 Fick-based PVR vs. Cath-CMR-based PVR

As shown in Figure 2, total PVR estimated using the Fick-based method showed a significant difference compared to the PVR using the Cath-CMR method (Fick: 1.80 ± 0.77 iWU; Cath-CMR: 2.56 ± 1.36 iWU). On average, the Fick-based method produced PVR values approximately 0.75 iWU lower than those

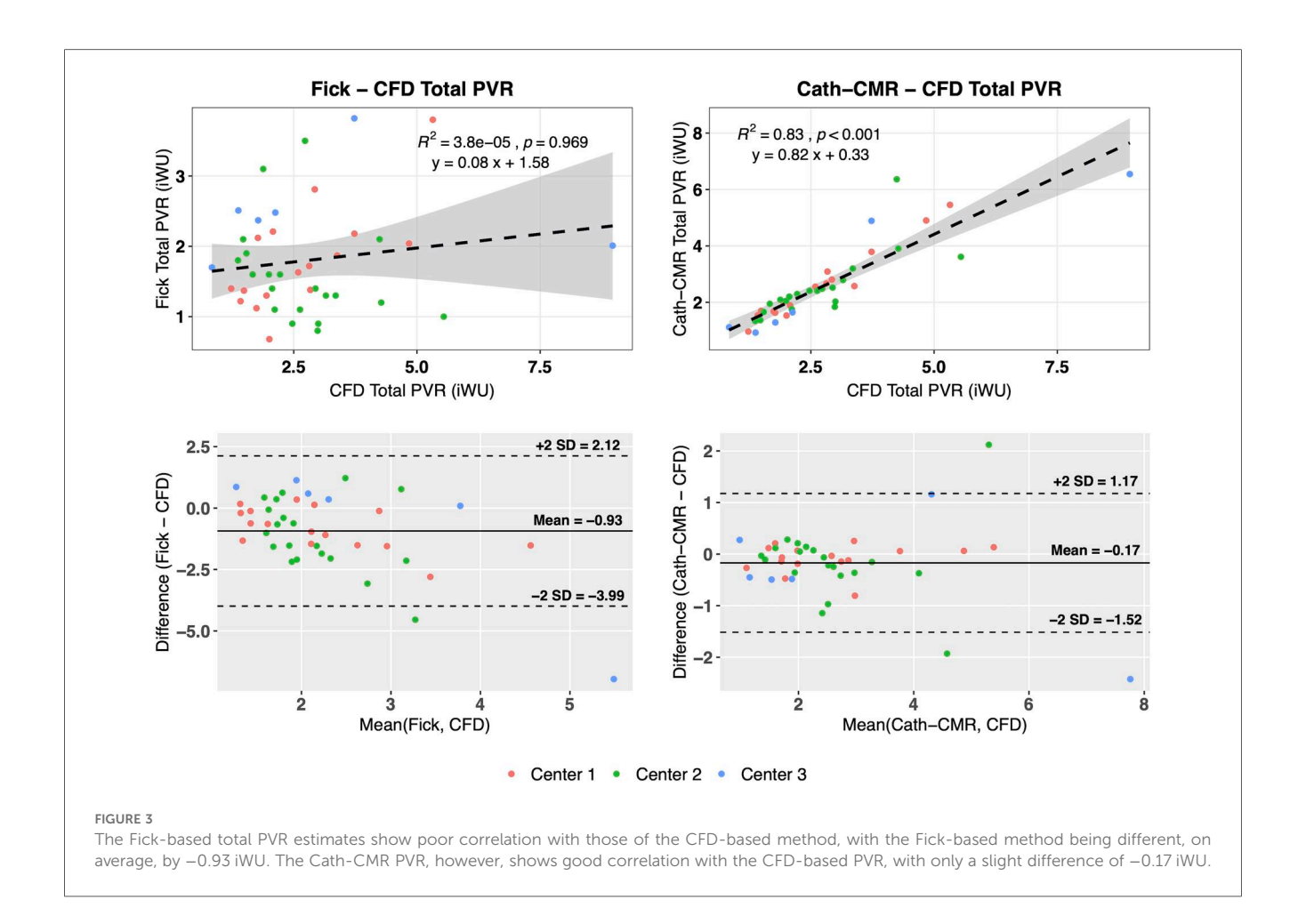
TABLE 1 Clinically measured mean flow and pressure values across three centers.

Center	N	Q _{SVC} (L/min)	Q _{LPA} (L/min)	Q _{RPA} (L/min)	P _{SVC} (mmHg)	P _{LPA} (mmHg)	P _{RPA} (mmHg)	P _{LA} (mmHg)	⊿P _L (P _{LPA} —P _{LA})	⊿P _R (P _{RPA} —P _{LA})
1	16	1.07 ± 0.26	0.52 ± 0.20	0.56 ± 0.17	9.31 ± 1.49	8.88 ± 1.54	9.00 ± 1.55	4.44 ± 0.96	4.44 ± 1.26	4.56 ± 1.26
2	20	1.11 ± 0.33	0.47 ± 0.14	0.67 ± 0.25	12.30 ± 1.34	11.45 ± 1.28	11.85 ± 1.31	7.65 ± 1.53	3.80 ± 1.06	4.20 ± 1.11
3	6	1.00 ± 0.16	0.49 ± 0.14	0.51 ± 0.10	11.83 ± 2.14	10.83 ± 2.48	11.33 ± 2.42	7.83 ± 2.14	3.00 ± 1.67	3.50 ± 1.76
P-value	-	0.854	0.820	0.100	< 0.001	< 0.001	< 0.001	< 0.001	0.066	0.333

A nonparametric Kruskal–Wallis test revealed a significant difference in pressure measurements, with the mean pressures for Center 1 being considerably lower than for Centers 2 and 3. However, no significant difference in left/right pressure gradients and flow measurements was observed across the three centers.



Comparison of total PVR between the three PVR estimation methods across all three centers indicates a significant difference between the Fickbased PVR and both the Cath-CMR and CFD-based PVR. In contrast, no statistical difference was found between the Cath-CMR-based PVR and CFD-based PVR.



obtained using the Cath-CMR method. Overall, the two methods demonstrated poor agreement with an ICC of 0.22 [p = 0.055; 95% CI: (-0.05, 0.47)].

3.3 CFD-based PVR estimation and comparison to Fick and Cath-CMR methods

For all three centers, individual left and right lung PVRs were computed using the CFD-based optimization algorithm. The resulting mean PVR was $\tilde{R}_{LPA} = 6.28 \pm 3.19 \text{ iWU}$ for the left lung and $\tilde{R}_{RPA} = 5.31 \pm 3.74$ iWU for the right lung, includes the proximal resistances 1.06 ± 1.26 iWU and $r_{RPA} = 0.66 \pm 0.69$ iWU for the left and right lung, respectively. Using Equations 3 and 4, the total PVR \tilde{R}_{total} was computed from \tilde{R}_{LPA} and \tilde{R}_{RPA} , yielding a mean $\tilde{R}_{total} = 2.73 \pm 1.48 \text{ iWU}$. As shown in Figure 3, poor agreement was observed between the Fick-based method and the CFD-based method [ICC = 0.10; p = 0.22; 95% CI: (-0.13, 0.34)], with the Fick method underestimating the total PVR of the CFD method by 0.93 iWU on average. In contrast, the CFD method showed much stronger agreement to the Cath-CMR method [ICC = 0.88; p < 0.001; 95% CI: (0.79, 0.93)], with the Cath-CMR method underestimating the total PVR of the CFD method by only 0.17 iWU. The

TABLE 2 Summary of mean total PVR estimates of the three methods.

Total PVR	Fick	Cath-CMR	CFD	<i>P</i> -value
Center 1	1.80 ± 0.75	2.55 ± 1.25	2.63 ± 1.20	0.057
Center 2	1.59 ± 0.70	2.51 ± 1.13	2.68 ± 1.07	< 0.001
Center 3	2.48 ± 0.73	2.74 ± 2.38	3.14 ± 3.02	0.587
P-value	0.017	0.531	0.452	

total PVR for all three methods and across all three centers is summarized in Table 2.

The mean individual PVRs (including proximal resistances) across all three centers using the CFD method were 6.28 ± 3.19 iWU for the left lung and 5.31 ± 3.74 iWU for the right lung. In comparison, the Cath-CMR method produced mean individual PVRs of 5.50 ± 2.91 iWU for the left lung and 5.26 ± 3.74 iWU for the right lung. It should be noted that the LPA resistance shows a larger discrepancy between the two methods, which can be attributed in part to the proximal resistances found in the CFD method, which were larger for the LPA $(1.06\pm1.26$ iWU) than for the RPA $(0.66\pm0.69$ iWU). Still, the two methods' individual PVR estimates show good agreement, with an ICC of 0.74 [p < 0.001; 95% CI: (0.56, 0.86)] for the left lung and an ICC of 0.95 [p < 0.001; 95% CI: (0.91, 0.97)] for the right lung. Similarly, as shown in Figure 4, the two methods show good correlation, particularly in the RPA,

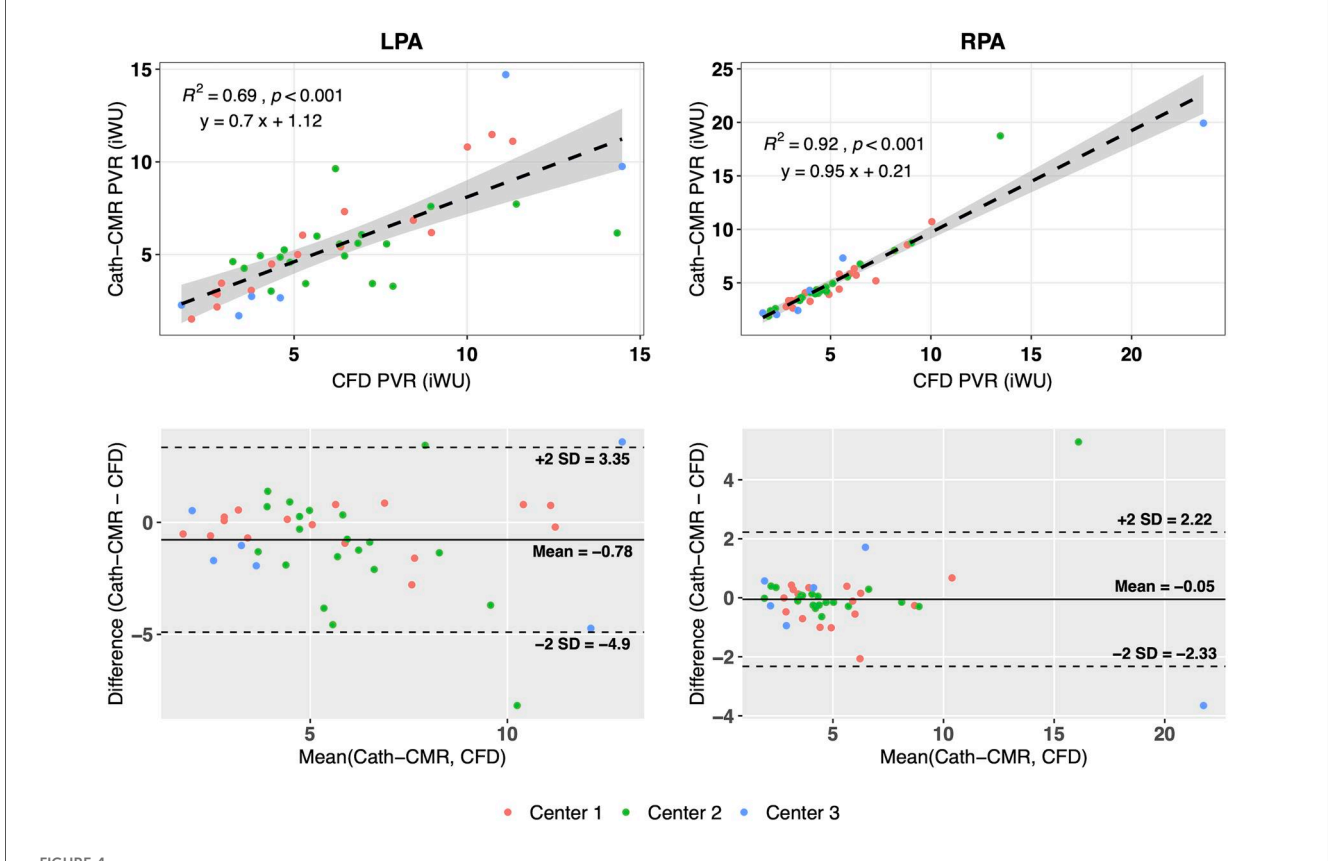


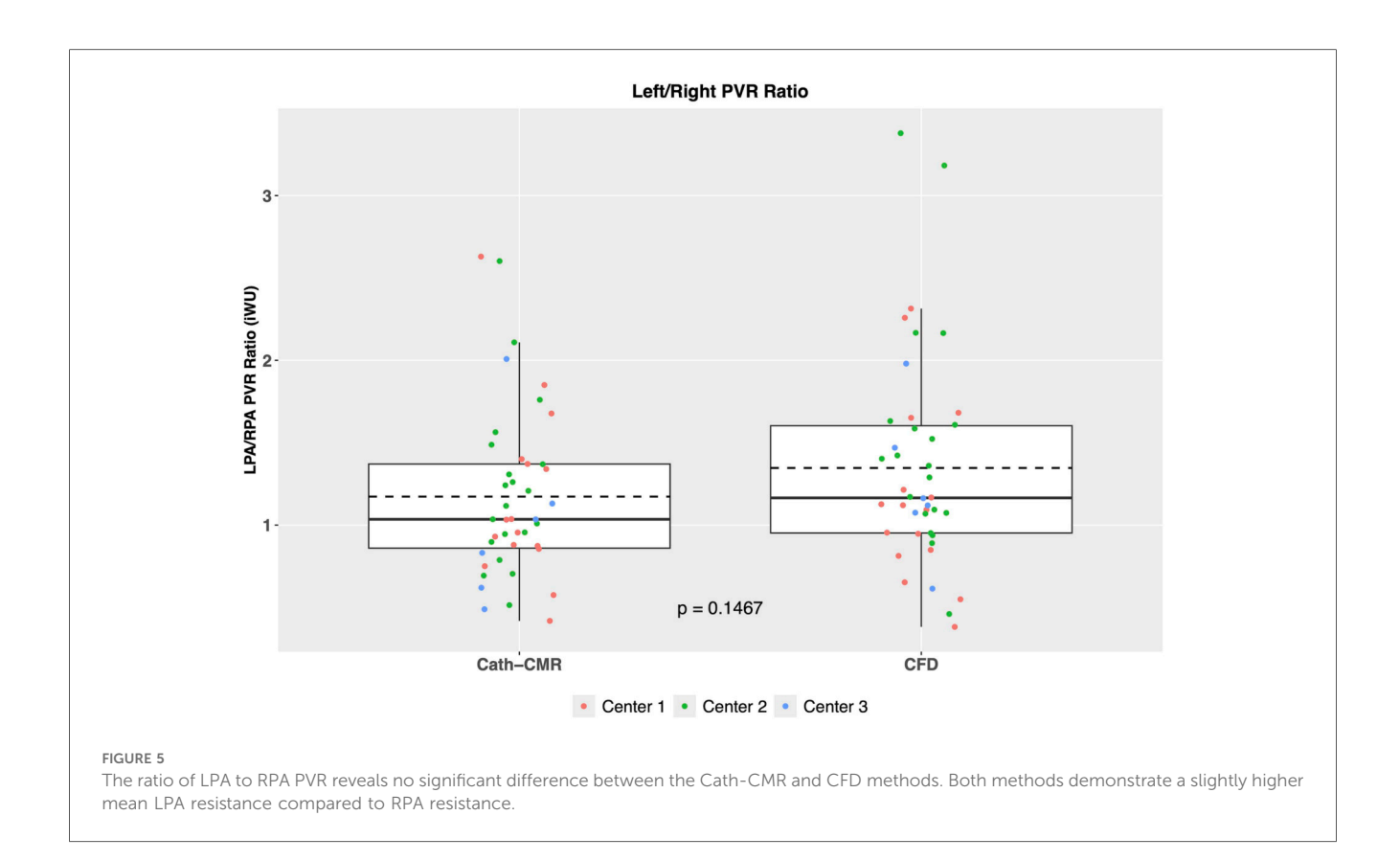
FIGURE 4
The individual lung resistances using the Cath-CMR method correlate well with those of the CFD method, particularly for the RPA. However, the Cath-CMR-based LPA PVR estimates show a bias of -0.78 iWU relative to the CFD-based LPA PVR, which is likely due to the increased proximal resistance in the LPA.

with the Cath-CMR-based PVR estimates underestimating the CFD-based PVR estimates by an average of 0.78 iWU for the left lung and 0.05 iWU for the right lung. The ratio of LPA and RPA resistance also indicates no significant difference between the individual lung PVR estimates of the Cath-CMR method and the CFD method, with a mean LPA/RPA ratio of 1.17 ± 0.52 for the Cath-CMR method and 1.35 ± 0.64 for the CFD method, as shown in Figure 5.

4 Discussion

This three-center study on PVR estimation in children with Glenn vasculature reveals two important findings. First, there are substantial discrepancies in total PVR estimates between the Fick-based method and both the Cath-CMR and CFD methods. Several factors may contribute to the discrepancies in total PVR. One source of possible error is in the calculation of the transpulmonary pressure gradient which, as seen in Equation 1, is computed as the difference in mPAP and PAWP, as measured by Cath. The PAWP measurement as a surrogate to direct LA pressure measurement has been shown to significantly overestimate LA pressure in pre-Fontan patients, resulting in an underestimation of PVR (23). Another source of possible error

lies in the limited interchangeability between pulmonary blood flow measured via the Fick principle and that measured by CMR, which has been shown in previous single-center studies (12, 13, 24, 25). One reason for this is the VO2 measurement in the calculation of Q_p in Equation 1, which can be particularly inaccurate for assumed VO2 estimates using formulas or tables based on age or weight (12). The discrepancies in PVR estimates between the Fick method and the other two methods are potentially significant because the Fontan risk stratification, which is based in part on PVR values, relies on these estimates. For instance, pulmonary hypertensive vascular disease (PHVD) serves as an indicator of Fontan failure. The threshold for PHVD (and an elevated risk of Fontan failure) is a mean transpulmonary pressure gradient exceeding 6 mmHg or an indexed PVR surpassing 3 iWU for single ventricle physiology (26). Using this threshold, the Fick-based method classifies 36 cases as normal risk, while the CFD method classifies only 29 as normal, as illustrated in Figure 6. Of the remaining six cases which were classified as elevated risk by the Fick method, only four were also classified as such by the CFD method. Overall, the Fick-based method demonstrated an agreement of 78.6% with the CFD method in terms of PHVD risk classification. In contrast, the Cath-CMR method demonstrated a classification agreement of 92.9% with the CFD method. However, even a 7%

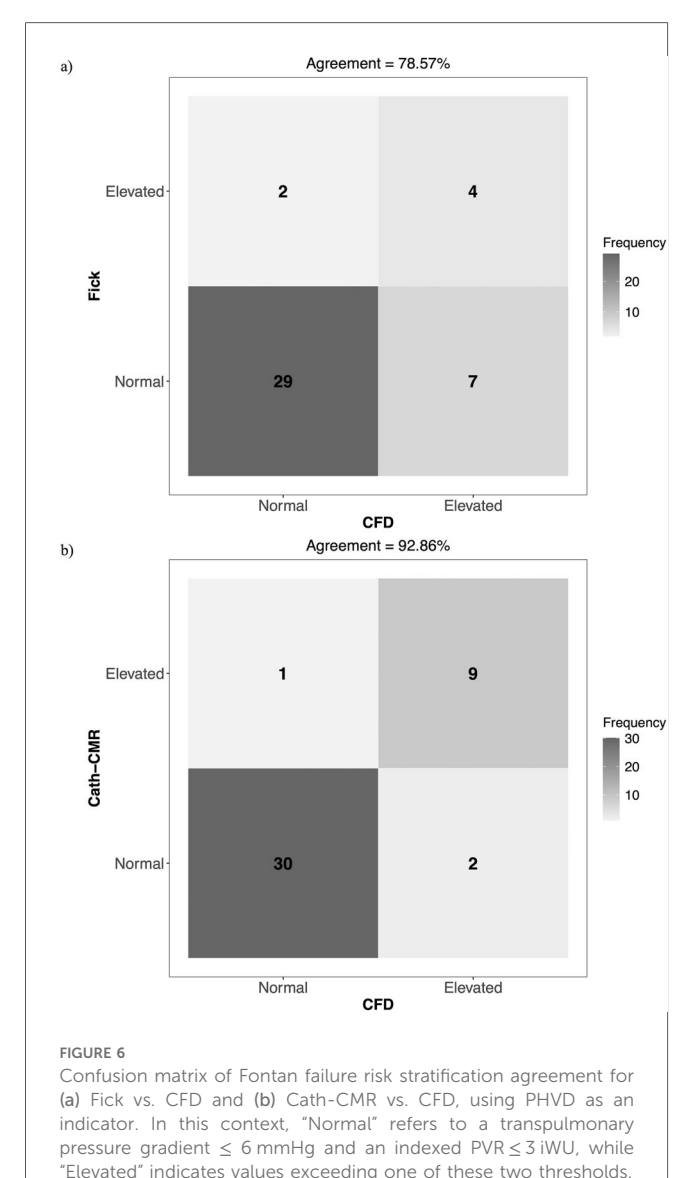


PHVD misclassification poses a risk of performing Fontan surgery on high-risk cases that may not be suitable for the procedure. For instance, misclassifying a patient as low-risk and proceeding with the Fontan procedure could lead to complications such as high central venous pressure, low cardiac output, or pleural effusion. Conversely, erroneously classifying a patient as high-risk may unnecessarily delay the Fontan procedure to start a new medication.

The second finding is that the proximal resistances included in the CFD method significantly contribute to the PVR, particularly for the LPA. As shown in Figure 4, the correlation between Cath-CMR-based LPA PVR and CFD-based PVR is significantly lower than for the RPA, along with a much higher bias. This discrepancy is likely attributed to the increased proximal resistance exhibited by the CFD method in the LPA $(1.06 \pm 1.26 \text{ iWU})$, which is significantly greater than that of the RPA ($0.66 \pm 0.69 \text{ iWU}$). The increased LPA proximal resistance is understandable, as the LPA outlet surface area in the CFD models is on average smaller than that of the RPA, with a mean of 0.50 ± 0.39 cm² for the LPA and $0.58 \pm 0.32 \text{ cm}^2$ (p = 0.069). This is attributable to anatomical factors such as the large Damus-Kaye-Stansel anastomosis performed during the Norwood operation, which often rests on the proximal LPA, exerting external compression and narrowing the vessel. Another possible factor contributing to the discrepancy in proximal resistance between the LPA and RPA is their length. In our future research, we plan to investigate the impact of pulmonary artery length on proximal resistance. However, we anticipate that this effect will be less pronounced compared to the influence of the pulmonary arterial radius. This is because the models of pulmonary arteries are roughly cylindrical in shape, which means that resistance increases linearly with vessel length while it exhibits an inverse fourth-order relationship with the pulmonary arterial radius.

Overall, the CFD method for estimating PVR may be advantageous to both the Fick and Cath-CMR methods. First, it allows the determination of individual lung resistances, something that is not typically done with the Fick method. Second, it does not rely on Q_p measurements derived from VO_2 measurements and arteriovenous oxygen content. Instead, it uses Q_p measured by CMR, which is the gold standard for pulmonary blood flow measurement. Finally, the CFD method offers a more complete representation of pulmonary resistances compared to the Cath-CMR method, as it incorporates both distal and proximal resistances in the LPA and RPA.

However, several limitations must be acknowledged. First, the CFD PVR estimation algorithm has only been tested using a simplified model of the Glenn vasculature. It does not currently account for vessel wall compliance or variations in blood viscosity, both of which may influence resistance and should be explored in future work using more realistic models. Including compliance in the CFD model would allow for a more accurate optimization to the clinical flow curves by adding an additional parameter for exploration. However, the introduction of an additional optimization parameter may lead to issues in identifiability (27, 28), which warrants further exploration alongside model compliance in future studies. An alternative approach to conducting an identifiability analysis is to approximate compliance directly from distensibility (29), thereby



avoiding potential issues of identifiability associated with the introduction of compliance. Incorporating compliance may also enable more precise pressure wave dynamics, which may affect the transpulmonary pressure gradient used in the CFD optimization (30). Blood viscosity is generally assumed to be Newtonian in large vessels such as the pulmonary arteries (31), so it is not expected to impact PVR significantly. However, if the model was extended further into the lungs where vessel size decreases significantly, blood viscosity should be modeled as non-Newtonian.

Second, the sample size was limited to fewer than 50 patients. A larger cohort would enhance the statistical power and generalizability of the findings, which is particularly important for determining the concordance between Fontan risk classifications and PVR estimation methods. An increased sample size would also improve the reliability of ICC estimates and allow for more meaningful subgroup analyses.

Third, the timing between Cath and CMR exams varied among patients. Some underwent both procedures on the same

day, while others had them separated by up to a year, potentially introducing temporal variability in the measurements. However, since most patients had their Cath and CMR exams on the same day, no significant differences in the statistical conclusions are expected. As the sample size grows in future studies, it would be intriguing to observe the impact of temporal misalignment between Cath and CMR exams.

Finally, the Cath-CMR and CFD methods neglected to consider collateral flow. However, it is anticipated that the presence of collateral flow would have a similar impact on the Fick, Cath-CMR, and CFD methods, causing them to underestimate the total pulmonary flow and consequently leading to an increased PVR. Given these limitations, further clinical study is needed to determine which PVR method most effectively correlates with clinical outcomes.

5 Conclusion

The comparison of methods for computing PVR revealed inconsistencies between the Fick-based method and both the Cath-CMR and CFD methods in patients with Glenn physiology, as observed across three centers. The CFD-based computational optimization method for PVR estimation demonstrated excellent agreement with the Cath-CMR method for RPA PVR estimation, but only modest agreement in LPA PVR estimation. This underscores the significance of considering both proximal and distal lung resistance, potentially making the CFD method more suitable than the Cath-CMR method. Further research is warranted to determine which method represents the most accurate quantification of PVR in pre-Fontan patients.

Data availability statement

The data analyzed in this study is subject to the following licenses/restrictions: Data cannot be shared publicly because of the policies of Children's Hospital Colorado, Children's National Hospital, and West Virginia University Medicine Children's Hospital. Data are available from the respective ethics committees for researchers who meet the criteria for access to confidential data. Requests to access these datasets should be directed to; Heather Byrd, heather.byrd@cuanschutz.edu; Yue-Hin Loke, YLoke@childrensnational.org; Candie DaFonzo, candace.dafonzo@wvumedicine.org.

Ethics statement

The studies involving humans were approved by West Virginia University Institutional Review Board Protocol 2410047107. The studies were conducted in accordance with the local legislation and institutional requirements. The ethics committee/institutional review board waived the requirement of written informed consent for participation from the participants

or the participants' legal guardians/next of kin because of the anonymized, retrospective nature of the study.

Author contributions

SL: Visualization, Writing – original draft, Software, Formal analysis, Conceptualization, Validation, Investigation, Writing – review & editing, Methodology. DC: Data curation, Resources, Writing – review & editing, Data curation. CM: Writing – review & editing, Resources, Data curation. JU: Data curation, Writing – review & editing, Resources. BF: Resources, Data curation, Writing – review & editing. JR: Writing – review & editing, Resources, Data curation. Y-HL: Writing – review & editing, Data curation, Resources. VK: Writing – review & editing, Methodology, Investigation, Conceptualization, Formal analysis. MM: Formal analysis, Project administration, Investigation, Supervision, Methodology, Writing – review & editing, Conceptualization, Funding acquisition.

Funding

The author(s) declare that financial support was received for the research and/or publication of this article. This project is funded and supported by a grant from the National Institute of Health-National Heart, Lung, and Blood Institute (R01HL149807).

References

- 1. Fontan F, Baudet E. Surgical repair of tricuspid atresia. *Thorax.* (1971) 26(3):240-8. doi: 10.1136/thx.26.3.240
- 2. De Leval MR, Kilner P, Gewillig M, Bull C, McGoon DC. Total cavopulmonary connection: a logical alternative to atriopulmonary connection for complex Fontan operations: experimental studies and early clinical experience. *J Thorac Cardiovasc Surg.* (1988) 96(5):682–95. doi: 10.1016/S0022-5223(19)35174-8
- 3. Petit CJ. Staged single-ventricle palliation in 2011: outcomes and expectations. Congenit Heart Dis. (2011) 6(5):406-16. doi: 10.1111/j.1747-0803.2011.00560.x
- 4. Chowdhury UK, Airan B, Kothari SS, Talwar S, Saxena A, Singh R, et al. Specific issues after extracardiac Fontan operation: ventricular function, growth potential, arrhythmia, and thromboembolism. *Ann Thorac Surg.* (2005) 80(2):665–72. doi: 10. 1016/j.athoracsur.2005.02.024
- 5. Gentles TL, Mayer JE, Gauvreau K, Newburger JW, Lock JE, Kupferschmid JP, et al. Fontan operation in five hundred consecutive patients: factors influencing early and late outcome. J Thorac Cardiovasc Surg. (1997) 114(3):376–91. doi: 10.1016/S0022-5223(97)70183-1
- Khiabani RH, Whitehead KK, Han D, Restrepo M, Tang E, Bethel J, et al. Exercise capacity in single-ventricle patients after Fontan correlates with haemodynamic energy loss in TCPC. Heart. (2015) 101(2):139–43. doi: 10.1136/ heartjnl-2014-306337
- 7. Duncan BW, Desai S. Pulmonary arteriovenous malformations after cavopulmonary anastomosis. *Ann Thorac Surg.* (2003) 76(5):1759–66. doi: 10.1016/S0003-4975(03)00450-8
- 8. Shah MJ, Rychik J, Fogel MA, Murphy JD, Jacobs ML. Pulmonary AV malformations after superior cavopulmonary connection: resolution after inclusion of hepatic veins in the pulmonary circulation. *Ann Thorac Surg.* (1997) 63(4):960–3. doi: 10.1016/S0003-4975(96)00961-7
- 9. Dave A, Santos RD, Siddiqi U, Dharia A, Li W, Siddiqi U, et al. Applications of computational fluid dynamics in congenital heart disease: a review. *J Cardiovasc Dev Dis.* (2025) 12(2):70 doi: 10.3390/jcdd12020070
- 10. Frieberg P, Aristokleous N, Sjöberg P, Töger J, Liuba P, Carlsson M. Computational fluid dynamics support for fontan planning in minutes, not hours:

Conflict of interest

The authors declare that the research was conducted in the absence of any commercial or financial relationships that could be construed as a potential conflict of interest.

Generative AI statement

The author(s) declare that no Generative AI was used in the creation of this manuscript.

Any alternative text (alt text) provided alongside figures in this article has been generated by Frontiers with the support of artificial intelligence and reasonable efforts have been made to ensure accuracy, including review by the authors wherever possible. If you identify any issues, please contact us.

Publisher's note

All claims expressed in this article are solely those of the authors and do not necessarily represent those of their affiliated organizations, or those of the publisher, the editors and the reviewers. Any product that may be evaluated in this article, or claim that may be made by its manufacturer, is not guaranteed or endorsed by the publisher.

the next step in clinical Pre-interventional simulations. *J Cardiovasc Transl Res.* (2022) 15(4):708–20. doi: 10.1007/s12265-021-10198-6

- 11. Rosenzweig EB, Abman SH, Adatia I, Beghetti M, Bonnet D, Haworth S, et al. Paediatric pulmonary arterial hypertension: updates on definition, classification, diagnostics and management. *Eur Respir J.* (2019) 53(1):1801916. doi: 10.1183/13993003.01916-2018
- 12. Downing TE, Whitehead K, Dori Y, Gillespie M, Harris M, Fogel M, et al. Accuracy of conventional oximetry for flow estimation in patients with superior cavopulmonary connection: a comparison with phase-contrast cardiac MRI. *Circ Cardiovasc Imaging*. (2013) 6(6):943–9. doi: 10.1161/CIRCIMAGING.113.000496
- 13. Hart MR, Whiteside W, Yu S, Lowery R, Dorfman AL, Mahani MG, et al. Differences in pulmonary and systemic flow measurements by cardiac magnetic resonance vs cardiac catheterization and relation to collateral flow in single ventricle patients. *Pediatric Cardiol.* (2020) 41:885–91. doi: 10.1007/s00246-020-02327-w
- 14. Laudenschlager S, Schofield S, Drysdale N, Stone M, Romanowicz J, Frank B, et al. Estimation of pulmonary vascular resistance for Glenn physiology. *PLoS One.* (2024) 19(7):e0307890. doi: 10.1371/journal.pone.0307890
- 15. Wolf A, Pollman MJ, Trindade PT, Fowler MB, Alderman EL. Use of assumed versus measured oxygen consumption for the determination of cardiac output using the Fick principle. *Cathet Cardiovasc Diagn*. (1998) 43(4):372–80. doi: 10.1002(sici) 1097-0304(199804)43:4<372::aid-ccd3>3.0.co;2-5
- 16. Shanahan CL, Wilson NJ, Gentles TL, Skinner JR. The influence of measured versus assumed uptake of oxygen in assessing pulmonary vascular resistance in patients with a bidirectional Glenn anastomosis. *Cardiol Young.* (2003) 13(2):137–42. doi: 10.1017/S1047951103000271
- 17. Updegrove A, Wilson NM, Merkow J, Lan H, Marsden AL, Shadden SC. Simvascular: an open source pipeline for cardiovascular simulation. *Ann Biomed Eng.* (2017) 45(3):525–41. doi: 10.1007/s10439-016-1762-8
- 18. Shapiro SS, Wilk MB. An analysis of variance test for normality (complete samples). *Biometrika*. (1965) 52(3–4):591–611. doi: 10.1093/biomet/52.3-4.591
- 19. Kruskal WH, Wallis WA. Use of ranks in one-criterion variance analysis. J Am Stat Assoc. (1952) 47(260):583–621. doi: 10.1080/01621459.1952.10483441

- 20. Wilcoxon F. Individual comparisons by ranking methods. Biometrics Bulletin. (1945) 1(6):80–3. doi: 10.2307/3001968
- 21. Fisher R. Statistical Methods for Research Workers. Edinburgh: Oliver & Boyd (1925).
- 22. Bland JM, Altman DG. Statistical methods for assessing agreement between two methods of clinical measurement. *Lancet*. (1986) 327(8476):307–10. doi: 10.1016/S0140-6736(86)90837-8
- 23. Bernstein FJ, Badran S, Takao C. Relationship of pulmonary artery wedge pressure to left atrial pressure and pulmonary vascular resistance in preoperative Fontan patients. *Pediatr Cardiol.* (2012) 33:15–20. doi: 10.1007/s00246-011-0057-y
- 24. Langanecha B, Chaturvedi R, Seed M, Lam CZ, Yoo S-J. Fick's versus cardiac MRI measured pulmonary blood flow in Pre-Fontan assessment. *Circulation*. (2022) 146:A11006–A11006. doi: 10.1161/circ.146.suppl_1.11006
- 25. Mendonsa E, Patel N, Detterich J. Comparison of hemodynamics using combined cardiac catheterization and cardiac magnetic resonance data a single center experience. *J Cardiovasc Magn Reson.* (2025) 27. doi: 10.1016/j.jocmr.2024.101527
- 26. Hansmann G, Koestenberger M, Alastalo TP, Apitz C, Austin ED, Bonnet D, et al. 2019 updated consensus statement on the diagnosis and treatment of pediatric pulmonary hypertension: the European pediatric pulmonary vascular

- disease network (EPPVDN), endorsed by AEPC, ESPR and ISHLT. J Heart Lung Transplant. (2019) 38(9):879–901. doi: 10.1016/j.healun.2019.06.022
- 27. Colebank MJ, Chesler NC. An in-silico analysis of experimental designs to study ventricular function: a focus on the right ventricle. *PLoS Comput Biol.* (2022) 18(9):e1010017. doi: 10.1371/journal.pcbi.1010017
- 28. Raue A, Kreutz C, Maiwald T, Bachmann J, Schilling M, Klingmüller U, et al. Structural and practical identifiability analysis of partially observed dynamical models by exploiting the profile likelihood. *Bioinformatics*. (2009) 25(15):1923–9. doi: 10.1093/bioinformatics/btp358
- 29. Wang Z, Chesler NC. Pulmonary vascular wall stiffness: an important contributor to the increased right ventricular afterload with pulmonary hypertension. *Pulm Circ.* (2011) 1(2):212–23. doi: 10.4103/2045-8932.83453
- 30. Tang E, Wei ZA, Fogel MA, Veneziani A, Yoganathan AP. Fluid-structure interaction simulation of an intra-atrial Fontan connection. *Biology (Basel)*. (2020) 9(12):412. doi: 10.3390/biology9120412
- 31. Kheyfets VO, O'Dell W, Smith T, Reilly JJ, Finol EA. Considerations for numerical modeling of the pulmonary circulation—a review with a focus on pulmonary hypertension. *J Biomech Eng.* (2013) 135(6):61011–15. doi: 10.1115/1. 4074141